

Synthesis, Characterization, and Fiber Studies of Certain Aromatic Polyamides

M. BALASUBRAMANIAN, M. J. NANJAN,* and M. SANTAPPA,
Department of Physical Chemistry, University of Madras, Madras 600025, India

Synopsis

Three aromatic polyamides containing alkyl and ether linkages in the main chain were synthesized, using low-temperature solution and interfacial polycondensation procedures, and were characterized by viscosity, solubility, UV, IR, TGA, and DSC studies. Fibers were spun using a laboratory-scale wet spinning unit and their mechanical and morphological properties studied. The results were correlated with structure and spinning conditions.

INTRODUCTION

As aromatic polyamides are generally intractable, attention has been given in recent times to the introduction of flexible linkages into the polymer chain.¹⁻³ Incorporation of alkyl groups has been shown to increase the solubility, though with a decrease in thermal stability.⁴ Introduction of aromatic ether linkage into the polymer backbone is known to impart processability to the polymer with a little reduction in thermal stability.^{5,6} Our earlier reports describe the synthesis of certain new thermally stable aromatic polyamides from a diamine preformed with both alkyl and aromatic ether linkages.⁷⁻⁹ In this article, we report the synthesis of three such aromatic polyamides using a modified low-temperature polycondensation techniques. These polyamides are characterized by viscosity, solubility, UV, IR, TGA, and DSC and the properties correlated with structure. Fibers spun from these polymers by wet spinning are characterized by tensile and morphological studies and the results correlated with the structure of the polymers and spinning conditions.

EXPERIMENTAL

Materials

2,2-Bis[4-(*p*-aminophenoxy)phenyl]propane, the diamine preformed with isopropylidene and aromatic ether linkage, was prepared from *p*-chloronitrobenzene and bisphenol A. The detailed procedure adopted has been already reported.^{7,9} The diamine was recrystallized from benzene (mp 124°C). 4,4'-Azodibenzoic acid was prepared by the reductive coupling of 4-nitrobenzoic acid with glucose in alkaline medium.¹⁰ The diacid chlorides were prepared by refluxing the corresponding diacids with thionyl chlorides and recrystallizing from hexane. *N,N*-Dimethylacetamide (BDH, England) was distilled over P₂O₅ at a reduced pressure and stored over molecular sieves.

* To whom communications should be addressed.

The polymerizations were carried out by both low-temperature solution and interfacial polycondensation methods.¹¹ As the aromatic diamine employed, 2,2-bis[4-(*p*-aminophenoxy)phenyl]propane, was not soluble in water, the interfacial procedure adopted by Morgan for water-insoluble diamine was adopted.¹¹ In this method, one equivalent of the diamine with one equivalent of sodium carbonate (acid acceptor) and sodium laurylsulfate (surfactant) dispersed in a CHCl_3 /water mixture was stirred in nitrogen atmosphere at room temperature. A solution of one equivalent of diacid chloride in chloroform was then added at once with rapid stirring. After 10 min, hexane was added and the precipitated polymer was filtered, washed, and dried over P_2O_5 at 100°C under vacuum.

In solution polymerization, certain modifications were made to increase the molecular weight.¹²⁻¹⁵ A reaction kettle was specially constructed with a stainless steel bottom and stirrer to bring down the sudden rise in temperature produced on the addition of acid chloride powder by an efficient heat transfer mechanism. A Teflon stirring guide was used to achieve a higher stirring rate.

The reactants were purified just prior to the reaction. The difficulty in adding the acid chloride powder into the reaction kettle was overcome by adding it from a test tube kept inside a rubber balloon which was connected to the reaction kettle. The concentration of the monomers were adjusted to obtain dopes with a polymer content of approximately 5–7%. One equivalent of the diamine was stirred in DMAc containing 5% LiCl in nitrogen atmosphere at -10 to -5°C . After 15 min of stirring, one equivalent of powdered diacid chloride was added with rapid stirring. After 30 min of further stirring, the ice-salt bath was removed and the contents were allowed to attain room temperature slowly over 2 hr. One equivalent of Li_2CO_3 was then added with stirring and the contents were left overnight. The polymer precipitated in water was filtered, washed, and dried over P_2O_5 at 100°C under vacuum.

Characterization

The inherent viscosity of the polymer solutions in DMAc containing 5% LiCl at 25°C at a concentration of 0.5 g/dl was determined with Ubbelohde suspended-type viscometer. Solubility of the polymer samples in various solvents was determined. UV-visible spectra of the polymer samples were recorded with Carl Zeiss UV-VIS Specord in concentrated H_2SO_4 (98% AR) in a closed cell at room temperature. IR spectra of the polymer films cast over a mercury bed were recorded with a Beckman IR 20 spectrophotometer. Thermal degradation of the polymer samples was studied by dynamic thermogravimetry with a Stanton Redcroft TG 750 thermobalance, at a heating rate of $10^\circ\text{C}/\text{min}$ in nitrogen or oxygen atmosphere. DSC curves were obtained with a Perkin-Elmer DSC 1B at a heating rate of $16^\circ\text{C}/\text{min}$ in nitrogen atmosphere for the polymer samples crimped in an aluminum sample pan.

Fiber Studies

Fibers were spun from the polymer dopes (about 10–15%) in DMAc using a laboratory-scale wet spinning unit. DMAc containing 5% LiCl was used as the solvent for the polyamide containing azo linkage. DMAc solution, 10% (v/v),

at room temperature was used as the coagulation bath. The fibers were washed, dried, and hot stretched. The tensile properties of the fibers were determined with an Instron tensile strength testing machine.

Fiber cross sections were investigated with a Cambridge Stereoscan model S-4-10 scanning electron microscope. Wide-angle X-ray Scattering (WAXS) patterns of the fibers were recorded with a flat film camera fitted to an X-ray generator (RADON HOUSE, INDIA). A nickel-filtered $\text{CuK}\alpha_1$ 1.54 Å radiation was employed.

RESULTS AND DISCUSSION

The structures and their codes of the polyamides synthesized are given in Figure 1. Although the addition of Li_2CO_3 to the polymerization mixture increases the molecular weight, the exact time of addition seems to be significant. Lowest viscosities were observed for the polymers precipitated without the addition of Li_2CO_3 . There was an increase in viscosity when the reaction mixture was kept for 12 hr. This may be explained by the later stages of condensation of unreacted polymer chain ends that takes place slowly due to the highly viscous nature of the reaction medium. Highest molecular weight was achieved when the reaction mixture was kept for 12 h after the addition of Li_2CO_3 . This may be due to the fact that the LiCl salt produced on the neutralization process forms an amide- LiCl salt-solvent complex which is a better solvating system than neat amide solvent or the amide-hydrochloride solvent mixture formed during the course of the reaction.

Generally, the solution method gives higher η_{inh} values than the interfacial method (Table I). The difference in viscosities observed among the polymers may be explained in terms of the relative rigidity of the polymer backbone. The lowest viscosity of 0.8 dl/g observed for PAEI may be explained as due to the meta-oriented benzene ring present in the polymer backbone that reduces the rigidity and hence the effective volume. The higher η_{inh} values observed for PAET and PAEI (1.1 and 0.82 dl/g, respectively) compared to the earlier reports

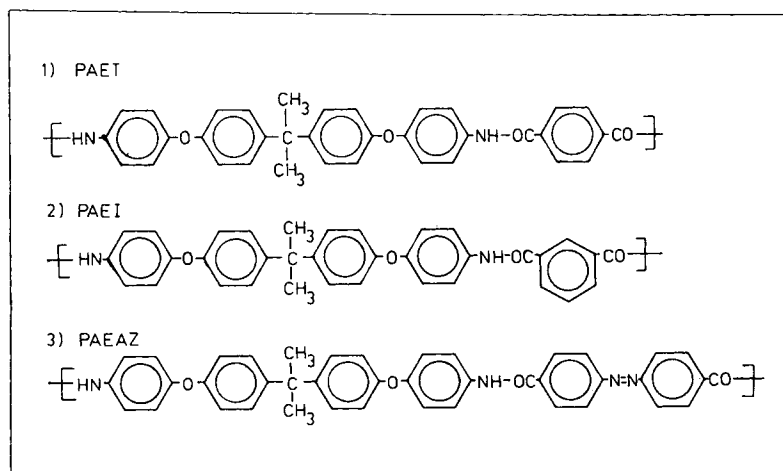


Fig. 1. Structure of polyamides with the codes.

TABLE I
 Properties of Polymers

Polymer	Polymerization method				Color	T_{\max}^b °C	IR Stretching frequencies, cm^{-1}	
	Solution		Interfacial				C=O	NH
	Yield, %	η_{inh}^a	Yield, %	η_{inh}^a				
PAEI	89	0.82	85	0.44	White	585	1655	3250
PAET	87	1.10	96	0.43	White	575	1645	3300
PAAEZ	85	1.89	87	0.43	Yellow	535	1645	3300

^a Inherent viscosity in DMAc/LiCl at 25°C, concn. 0.5 g/dl.

^b Temperature at which the rate of decomposition is maximum.

(0.52 and 0.46 dl/g, respectively) may be attributed to the use of Li_2CO_3 as acid acceptor and DMAc containing LiCl salt as solvent. Earlier workers used propylene oxide as acid acceptor and neat DMAc as solvent.¹⁶

The solubilities of polymers in various solvents (Table II) can be correlated with the structure of the polymers. All three polyamides are soluble in amide-type solvents (with or without the added LiCl salt) and in concentrated H_2SO_4 . This solubility can be explained by the combined favorable effects of aromatic ether and isopropylidene linkages present in the polymer chain.^{16,17} The kink introduced into the polymer chain by the angle sustained by these linkages decreases the rigidity of the chain and hence increases the solubility. The solubility trend observed among the three polyamides (PAEI > PAET > PAAEZ) may be explained as due to the increase in rigidity as we go from PAEI to PAAEZ.

The UV-visible spectrum of PAAEZ is of interest because of the azochromophore present, and this has been already discussed by the authors.^{8,9} The IR spectra of the polyamides are given in Figure 2. In all the polyamides, the appearance of characteristic peaks at $1650 \pm 5 \text{ cm}^{-1}$ for amide carbonyl and $3275 \pm 25 \text{ cm}^{-1}$ for hydrogen-bonded amide groups confirms the formation of amide linkage. In the para-substituted polyamides PAET and PAAEZ, the carbonyl stretching frequency is observed at 1645 cm^{-1} . This is shifted to 1655 cm^{-1} in PAEI where the conjugation is affected by the meta-substituted benzene ring in the main chain.¹⁸ The peak around $2950 \pm 10 \text{ cm}^{-1}$ may be assigned to the isopropylidene group. The peak around $1230 \pm 5 \text{ cm}^{-1}$ may be assigned to the aromatic ether linkage.

The IR spectra of the PAET and PAAEZ are nearly superimposable, and it should be pointed out here that in aromatic azo compounds, specific assignments of the $-\text{N}=\text{N}-$ stretching is difficult because of the interference by the $-\text{C}=\text{C}-$ ring vibrations.¹⁹ The very small shifts observed at some peaks may

 TABLE II
 Polymer Solubility^a

Polymer	Solvent													
	Conc. H_2SO_4	TFA	<i>p</i> -Cresol	Pyri- dine	DMF-	DMF	LiCl	DMAc-	DMAc	LiCl	NMP-	NMP	LiCl	DMSO
PAEI	++	S	++	++	++	++	++	++	++	++	++	++	++	++
PAET	++	S	++*	--	++	++	++	++	++	++	++	++	++	++
PAAEZ	++	-	S	--	++	++	++	++	++	++	++	++	++	++

^a ++, Soluble; S, swelling; --, insoluble; * soluble on heating with degradation.

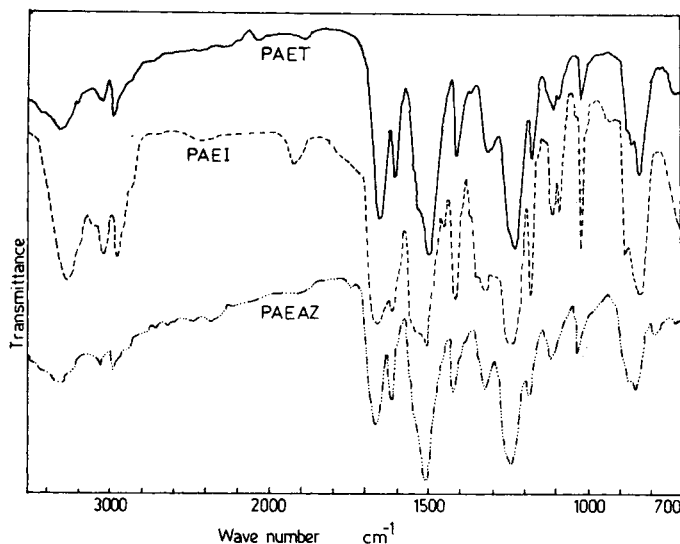


Fig. 2. IR spectra of the polymers.

be due to the +M effect of the lone pair of electrons on the nitrogen atom of the azo group para to the amide group.

The TGA curves of the polymers are given in Figure 3. To compare the thermal stabilities, the temperature at which the rate of decomposition is maximum (T_{\max}) is reported. Generally, the TGA curves of all the three polyamides show a small weight loss (about 5%) around 100–200°C, due to the loss of water absorbed by the polymers. A weight loss around 200°C is also likely due to the chain extension that may take place by the condensation of end groups resulting in the loss of a water molecule.²⁰ The higher thermal stabilities of these polymers as seen from its T_{\max} values may be explained as due to the thermally stable aryl ether linkage in the backbone. The higher T_{\max} values of PAET and PAEI (550°C) compared to earlier reports¹⁶ may be due to the higher molecular weights formed in the present study. The slightly lower T_{\max} value observed for PAEAZ compared to PAET and PAEI may be attributed to the presence of thermally less stable azo linkage.²¹ A comparison of the TGA of PAEAZ in nitrogen and oxygen atmosphere also indicates its low thermo-oxidative stability. The DSC studies of PAEAZ have been discussed elsewhere.⁹ In the region 400–422°C, some exothermic transition was observed. The TGA of this sample in nitrogen atmosphere showed that a weight loss of 23% started around 440°C. This weight loss is higher than the nitrogen content of the azo group (4.3%). The transition observed in DSC at 400–422°C must therefore be associated with both the evolution of nitrogen and some oxidized products, combined with trans → cis isomerism which is shown by contraction in volume.^{22,23}

FIBER STUDIES

Data in Table III (Fig. 4) show that the tensile strength and modulus of the fibers are in the order PAEAZ > PAET > PAEI. This order may be explained in terms of the structure of the repeat unit and spinning conditions. Factors such as the extent of orientation of polymer molecules and the concentration

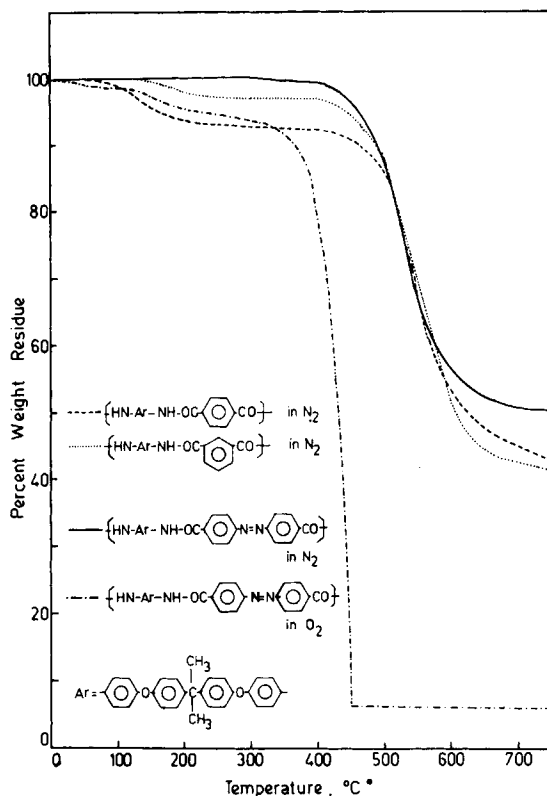


Fig. 3. TG curves of the polymers.

of voids formed in the fiber during spinning seem to decide the tensile properties.²⁴ The extent of orientation in aromatic polyamides is generally known to depend upon the number of para-linked benzene rings in the repeat unit. The extent of voids formation probably depends on the rate of coagulation. Rapid coagulation (rapid mass transfer) of the polymer dope, for instance, may result in high void concentration. The observation of low void formation in dry spinning and very little void formation in melt spinning of aliphatic polyamides strengthens this argument.²⁵

PAEI has the lowest number of para-substituted benzene rings. Further, it has the least packed superstructure among the polyamides because of the presence of meta-oriented benzene rings. This favors easier penetration of the nonsolvent molecules into the polymer dope and hence faster coagulation. This results in the formation of the highest void content leading to very poor tensile

TABLE III
Tensile Properties of the Fibers

Polymer	Stretch ratio	Draw ratio	Tenacity, g/denier	Elongation, %	Initial modulus, g/denier
PAEI	6.4	2	0.695	19.0	18.3
PAET	7.4	2.5	1.378	5.7	45.8
PAEAZ	33.5	2.6	1.488	4.6	75.0

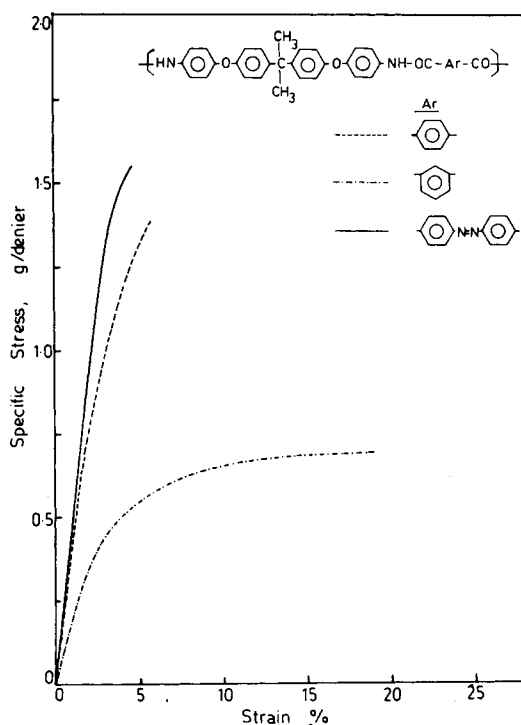


Fig. 4. Typical stress-strain diagram of the fibers.

properties. This is supported by the observation of large voids that are distributed throughout the cross section of the fiber, as seen from its SEM photographs (Fig. 6).

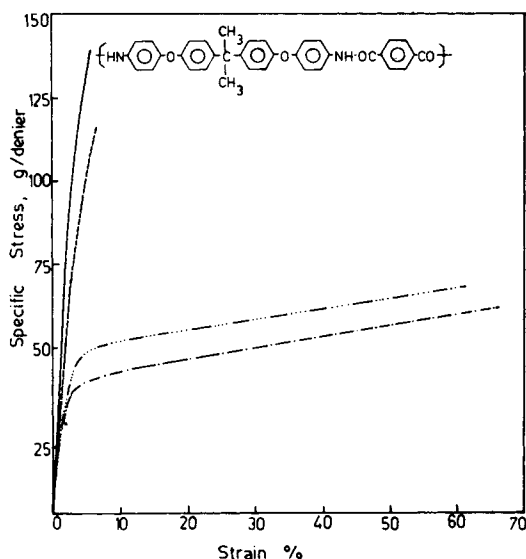


Fig. 5. Effect of hot drawing on stress-strain behavior: (---) as spun; (— · · —) 1.2; (---) 2.0; (—) 2.5.


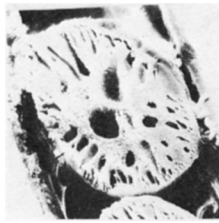
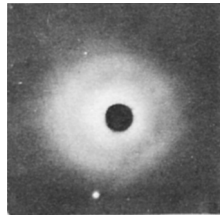


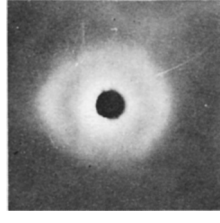


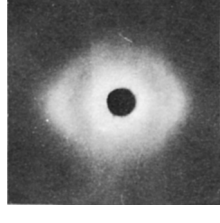
Polymer	SEM Photographs		WAXS Pattern
	as spun	hot drawn	
PAE I			
PAE T			
PAE AZ			

Fig. 6. SEM Photographs and WAXS patterns of the fibers.

Compared to PAEI, PAET has a more ordered and close-packed superstructure due to the presence of all para-substituted benzene rings. The rate of coagulation is therefore slower. The voids here are not only less concentrated than those observed in PAEI, but also a higher volume fraction of these voids is found in the annular than in the core part of the fiber. This is because the amount of nonsolvent that reaches the core of the fiber is less. In other words, the rate of coagulation decreases from the annular to the core. This explains the better tensile properties observed for PAET compared to PAEI.

The presence of the largest number of para-substituted benzene rings in PAEAZ favors highest orientation and hence greatest close packing among the three polyamides. Further, the larger distance between the two bulky isopropylidene groups in PAEAZ compared to the other two polyamides is an additional factor that favors close packing. Also the LiCl salt added to the polymer dope (to increase the solubility) stiffens the polymer chain and increases the orientation.²⁶ It also increases the polymer-solvent interaction and decreases the interaction between the polymer dope and the nonsolvent which further delays coagulation. All these factors favor a slow rate of coagulation resulting in very low void concentration as seen from the SEM photograph in Figure 6. This explains the highest tensile properties observed for this fiber.

For most of the fibers, higher stretch ratio seems to result in higher tensile properties. This may be due to the retention of orientation imparted by the

stretch at the face of the spinneret during coagulation.²⁵ Hot drawing of the as-spun fibers increases the tensile properties (Fig. 5) owing to the increase in orientation that results on stretching at higher temperatures. Hot drawing increases the tenacity and initial modulus at the expense of percentage of elongation at break. It is seen from SEM photographs (Fig. 6) that the voids are larger and better defined for hot-drawn than for undrawn fibers. This may be due to the expansion of air and solvent molecules trapped in the fibers.

The WAXS patterns of the fibers (Fig. 6) can also be correlated with the tensile properties (Table III). The development of arcs in the equatorial line with a background of diffused halo for the fibers of PAET and PAEAZ confirms that they have a certain amount of orientation along the fiber axis. PAEI, which has very little orientation, is seen to have only a diffused halo in its WAXS pattern and no arcs.^{27,28}

The authors thank Prof. V. B. Gupta, Dr. Veena, and Dr. Geetha of I.I.T. New Delhi for their help in fiber spinning and SEM photographs. One of the authors (M.B.) acknowledges University Grants Commission, India, for financial assistance.

References

1. G. F. L. Ehlers, Structure Stability Relationships of Polymers Based on Thermogravimetric Analysis Data, Parts I and II, AFML-TR-74-177, 1974.
2. W. Wright, *The Development of Heat Resistant Organic Polymers*, Wiley, New York, 1975, p. 43.
3. A. H. Frazer, *High Temperature Resistant Polymers*, Interscience, New York, 1968.
4. I. K. Verma, V. S. Sundari, and D. S. Varma, *J. Appl. Polym. Sci.*, **22**, 2857 (1978).
5. R. S. Lenk, J. L. White, and J. F. Feller, University of Tennessee, Polym. Sci. Eng. Rep. No. 56 and 58, 1975.
6. B. F. Malichenko, V. V. Sherikova, L. C. Chervgatsova, A. A. Kachan, and G. I. Motryuk, *Vysokomol. Soedin., Ser. B*, **14**, 423 (1972).
7. M. J. Nanjan, M. Balasubramanian, K. S. V. Srinivasan, and M. Santappa, *Polymer*, **18**, 411 (1977).
8. M. Balasubramanian, M. J. Nanjan, and M. Santappa, *Makromol. Chem.*, **180**, 2517 (1979).
9. M. Balasubramanian, M. J. Nanjan, and M. Santappa, *Makromol. Chem.*, **182**, 853 (1981).
10. M. C. Tomlison, *J. Chem. Soc.*, 756 (1946).
11. P. W. Morgan, *Condensation Polymers: By Interfacial and Solution Methods*, Interscience, New York, 1965.
12. J. Preston, W. B. Black, and W. C. Hofferbert, Jr., *J. Makromol. Sci. Chem.*, **A7**, 67 (1973).
13. H. Herlinger, H. P. Hoenner, F. Druchke, W. Denneles, and F. Haiber, *J. Appl. Polym. Symp.*, **21**, 201 (1973).
14. W. B. Black, *N.Y. Acad. Sci. (II)*, **32**, 765 (1970).
15. T. I. Bair, P. W. Morgan, and F. L. Killian, *Macromolecules*, **10**, 1396 (1977).
16. N. A. Glukhov, M. M. Koton, D. S. Ledneva, F. I. Nossova, L. M. Shcherbakova, and G. N. Fedarova, *Vysokomol. Soedin.*, **19**, 231 (1977).
17. Yu. N. Sazanova, G. N. Fedarov, L. M. Shcherbakova, and G. I. Nosova, *Polym. Sci. USSR*, **20**, 2487 (1979).
18. D. O. Hummel, *Polymer Spectroscopy*, Verlag Chemie, Weinheim, 1964, p. 112.
19. L. J. Bellamy, *The Infrared Spectra of Complex Molecules*, Chapman and Hall, London, 1975.
20. I. K. Verma, V. S. Sundari, and D. S. Varma, *J. Appl. Polym. Sci., Chem. Ed.*, **A7**, 325 (1973).
21. A. D. Delman, A. A. Stein, and B. B. Simms, *J. Macromol. Sci., Rev. Macromol. Chem.*, **1**, 147 (1967).
22. T. L. C. David and H. H. Morawetz, *Macromolecules*, **9**, 463 (1976).
23. D. Tabak and H. Morawetz, *Macromolecules*, **3**, 403 (1970).
24. R. S. Lenk, J. F. Feller, and J. L. White, *Polym. J.*, **9**, 9 (1977).

25. J. L. White and J. E. Spruiell, *Appl. Polym. Symp.*, **33**, 91 (1978).
26. M. Panar and L. F. Beste, *Macromolecules*, **10**, 1401 (1977).
27. L. E. Alexander, *X-Ray Diffraction Methods in Polymer Science*, Wiley-Interscience, New York, 1969, Chap. 4.
28. R. Meredith, *J. Text. Inst.*, **42**, T291 (1951).

Received February 12, 1981

Accepted August 25, 1981